Stability Diagram and Unfolding of a Modified Cytochrome *c*: What Happens in the Transformation Regime?

Harald Lesch,* Hans Stadlbauer,* Josef Friedrich,* and Jane M. Vanderkooi†

*Technische Universität München, Lehrstuhl für Physik Weihenstephan, 85350 Freising, Germany and †Department of Biochemistry and Biophysics, School of Medicine, The University of Pennsylvania, Philadelphia, Pennsylvania 19104 USA

ABSTRACT We determined the stability diagram of a modified cytochrome *c* protein in a glycerol water mixture by measuring the first and the second moment of the fluorescence from the chromophore as a function of temperature and pressure. Temperature and pressure were varied between 273 and 363 K and 0.0001 and 1 GPa, respectively. The shift of the fluorescence maximum showed a characteristic sigmoid-like pattern from which information on the microscopic processes during unfolding is obtained: as the transformation regime is entered, the fluorescence shows a significant blue shift. The conclusion is that water molecules get into contact with the chromophore. They lead to strong electrostatic contributions in the solvent shift, which counteract the red shifting dispersion interactions. Assuming that there are just two relevant states that determine the stability diagram, the complete set of thermodynamic parameters can be determined from the data. However, under certain pressure–temperature conditions the fluorescence pattern is more complicated, pointing toward reentrant transitions and, possibly, to consecutive steps in the unfolding process.

INTRODUCTION

The folding of proteins into a rather well-defined stable structure is one of the most important biomolecular processes. Its details, especially the respective kinetic aspects, are still not very well understood. However, also as to the thermodynamic aspects, there are more questions than answers. Because folding and unfolding under pressure and temperature variations are, for many proteins, especially for small ones, reversible processes, the unfolding process may shed light on what happens during the folding process. The present paper is aimed at unraveling some of the problems connected with the unfolding process of a modified cytochrome *c* (Cc) protein in a glycerol water mixture under quasi-static pressure and temperature variations.

An important aspect in this context concerns the so-called stability diagram of proteins, whose contour line separates the native state $N\rangle$ from the denatured state $D\rangle$ (Hawley, 1971; Zipp and Kauzmann, 1973; Heremans and Smeller, 1998). The shape of the diagram is ellipse-like, as first shown by Hawley. Strictly speaking, an elliptic shape is only obtained within the frame of a two-state model ($N\rangle$, $D\rangle$) and under the assumption that the second derivatives of the respective free enthalpies G are pressure- and temperature-independent quantities. This latter restriction implies that a protein is characterized by well-defined material parameters, namely a temperature- and pressure-independent specific heat, compressibility, and thermal expansion. Hence, the stability diagram contains the complete thermodynamics of the unfolding process of the protein under investigation, i.e., the differences ΔC_p, $\Delta\alpha$, $\Delta\beta$, ΔS, and ΔV where the Δ' denote the differences of the respective quantities in the native and the denatured state, respectively. However, to extract absolute numbers, one of the thermodynamic quantities should be known on an absolute scale. In our case, this additional information is obtained from a determination of the equilibrium constant as a function of pressure and temperature.

A thorough experimental validation of the quadratic approximation (elliptic shape) would imply the determination of the thermodynamic material parameters over a sufficiently large temperature and pressure range. From a practical point of view, this is not feasible because a nonlinear extrapolation into the respective unstable regions of the phase diagram would be necessary. Nevertheless, Makhatadze and Privalov (1995) performed such extrapolation studies for ΔC_p. Their results show that this quantity is fairly constant, say between 278 and 335 K, but may decay to zero far beyond the denaturation transition. Smeller and Heremans (1997) discussed in detail how a pressure and temperature dependence of the various parameters would change the shape of the diagram. The quadratic approximation seems to hold perfectly for liquid crystals (Clark, 1979). As to proteins, however, many experimental data show distortions of the elliptic shape. We stress that this does not necessarily reflect a failure of the approximations. Distortions may arise from a deviation from equilibrium due to the sometimes very long relaxation times. Another source of errors may be due to the very broad transformation ranges that lead to uncertainties in the determination of the respective thresholds. Despite these shortcomings, the data evaluation based on the quadratic approximation has yielded very reasonable values for the parameters involved. As we will show, this is true in our case as well.

An interesting problem concerns the transformation regime itself, namely the question as to what happens on a

Submitted July 18, 2001 and accepted for publication December 17, 2001.

Address reprint requests to Dr. Josef Friedrich, Technische Universität München, Lehrstuhl für Physik Weihenstephan, Vöttinger Str. 40, D-85350 Freising, Germany. Tel: +49-8161-71-3294; Fax: +49-8161-71-4517; E-mail: j.friedrich@lrz.tu-muenchen.de.

0006-3495/02/03/1644/10 $2.00

microscopic level at the boundary of the stability diagram. As to the thermal stability of proteins, this question was discussed by Baldwin (Baldwin, 1986; Baldwin and Muller, 1992). It was assumed that heat denaturation occurs under conditions where it becomes favorable for the protein to expose its hydrophobic core to the surrounding water solvent similar to how an oil droplet is dissolved in water. However, as Kauzmann (1987) pointed out, pressure denaturation of a protein does not fit into the concept of the oil droplet model, because the respective changes in volume have opposite signs. Recently, this discrepancy was solved by Hummer et al. (1998a,b). These authors suggested that, during pressure denaturation, quite in contrast to heat denaturation, water is pressed into the core of the protein where it fills the voids. During this process, the structure changes but only in a way that keeps the protein in its compact shape.

In this paper, we use fluorescence spectroscopy to shed some light on this problem. The quantity on which we focus is the center (λ_{max}) and the width (w) of the 00-transition of a chromophore within a protein. The chromophore used is a fluorescent derivative of the hemeprotein Cc. Fluorescence techniques are very useful in this context because, on the one hand, the band center and the width of a fluorescence line are very sensitive to changes in the molecular environment of the chromophore and, on the other hand, the interactions of a chromophore with its environment, which cause the changes in these quantities, are known in great detail so that information on what is happening on a microscopic level can be readily extracted from the respective experimental patterns.

EXPERIMENTAL

Materials aspects

Lyophilized substituted cytochrome *c* (Zn-Cc), in which zinc replaces the iron, was prepared from horse Cc (Sigma Chemical Co., St. Louis, MO) as previously described (Vanderkooi et al., 1976). It was dissolved in a mixture of KH_2PO_4-buffer at pH 7 and glycerol at a ratio of 1:2.5 (v/v). The protein concentration was 3.7×10^{-4} mol/l.

Spectroscopy

The solution (~25 nl) was filled into a diamond anvil cell. Pressure was varied between atmospheric pressure and ~1 GPa. Its magnitude was determined from the pressure shift of the ruby fluorescence whose reference values were taken from the literature (Eremets, 1996). The accuracy was ~100 MPa. The sample was excited with light from a pulsed dye laser pumped by an excimer laser. Excitation was carried out into the Soret band at 420 nm. The fluorescence light was collected in a collinear arrangement, dispersed in a spectrometer and detected via a CCD-camera. The resolution limit of the set-up was ~0.06 nm. The line center λ_{max} and the line width w (full-width half-maximum [FWHM]) of the 00-fluorescence band, the two quantities that we used for investigating protein stability, could be determined within an accuracy range of ~0.1 nm, respectively. This accuracy level amounts to ~3% of the total changes in these quantities. The experiments were carried out in a way that a certain temperature was kept constant and the pressure was varied or vice versa. The temperature could be controlled within an accuracy of ~0.5–2 K in a range covering 273 to 363 K.

A problem in the experiment concerns the establishing of thermal equilibrium. For some of the points in the stability diagram, we measured the respective kinetics, i.e., pressure and temperature in the transformation range were kept fixed, and the relaxation of the maximum of the fluorescence was measured. The respective relaxation times were in the range of 20 min. Hence, we adjusted the waiting times in the transformation range accordingly. Nevertheless, we stress that the establishing of thermal equilibrium may strongly depend on the thermodynamic conditions, and, because the transformation range is rather broad the question of how close to equilibrium the actual experiment was carried out is a serious one and not always easy to answer.

For the determination of the line shift and the line width, we proceeded in the following way. The main constituent of the chromophore is a rather rigid aromatic ring whose π-electron system determines the respective oscillator strength. Because this ring is not likely to be changed during the transformation, it is reasonable to assume that the oscillator strength of the transition considered does not change. In addition, the scale of the respective changes of the center and the width of the band is rather small as compared to the respective inhomogeneous width, e.g., a few nanometers compared to 15 nm, so that the total band could be reasonably well fitted by a Gaussian. Maximum and width of this Gaussian fit curve are the quantities that are plotted in the figures.

Determination of the equilibrium constant

For the following procedure, the assumption of thermal equilibrium for the whole transformation range is essential. As can be seen (e.g., see Figs. 2, 3, and 5), an increase of temperature and pressure results in a characteristic pattern of the shift of the band center. In the low range of these parameters, there is almost no shift or only a rather moderate red shift. The transformation range, in contrast, is characterized by a rather strong blue shift. After the transformation is completed, the blue shift levels off. As a rule, the transformation range is rather broad. This broad range may possibly be due to a low cooperativity of the transformation process or to a dispersion of the parameters involved. Along these lines of reasoning, we interpret the pattern of the shift of the band center in the following way (for details see Discussion). In the low (p, T)-parameter range, we just measure the pressure or temperature shift of the native state $|N\rangle$. We denote the wavelength just before transformation to the denatured state occurs, as λ_N. After the transformation is completed, we measure the respective shifts of the denatured state $|D\rangle$. We denote the wavelength associated with the denatured state just after the transformation is completed, as λ_D. λ_N and λ_D are determined from the intersections of the linearly extrapolated data ranges, as shown in Fig. 7. In the transformation range, the wavelength λ_{max} of the fluorescence maximum is a superposition of λ_N and λ_D weighted by the respective occupation probabilities p_N and p_D of the respective states. Suppose that the total band $F(\lambda)$ can be written as a superposition of two Gaussians:

$$F(\lambda) = p_N a_N \exp\left(\frac{-(\lambda - \lambda_N)^2}{2\sigma_N^2}\right) + p_D a_D \exp\left(\frac{-(\lambda - \lambda_D)^2}{2\sigma_D^2}\right). \quad (1)$$

Because, as argued above, the oscillator strengths a_N and a_D of the two states are roughly the same and the relative changes in the peak wavelength and the bandwidth are small, the exponentials are sufficiently similar, so

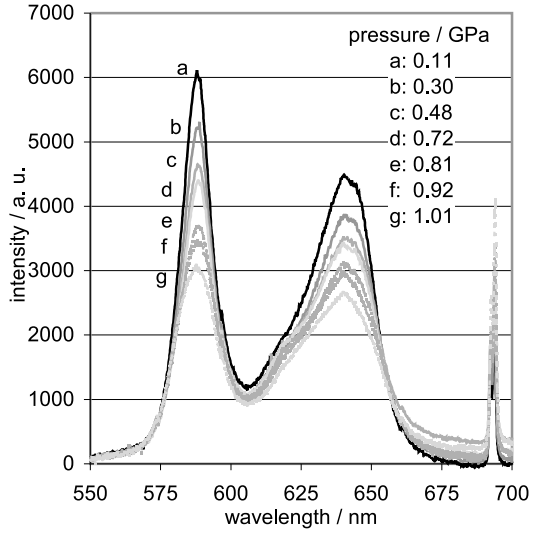

FIGURE 1 Fluorescence spectrum of Zn-Cc at ambient temperature. The band around 588 nm represents the Q_x-Q_y-00-band region. The band around 640 nm is a superposition of several vibronic bands. The narrow band around 695 nm is the fluorescence from ruby. The pressure levels at which the various spectra were taken are listed in the insert .

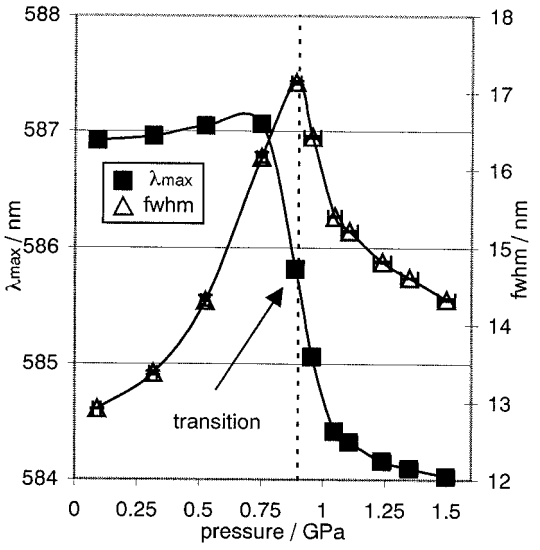

FIGURE 2 Center (λ_{max}) of the Q_x-Q_y-00-band and the respective width (FWHM) as a function of pressure measured at a temperature of 298 K. The stability boundary is indicated by the vertical broken line.

that the wavelength of the band maximum is obtained from the first derivative as

$$\lambda_{max} = p_N\lambda_N + p_D\lambda_D. \quad (2)$$

Within the frame of the two-state model, p_N and p_D can be expressed through the equilibrium constant K (Hawley, 1971; Vidugiris and Royer, 1998; Panick et al., 1999) as

$$p_N = \frac{1}{1+K}, \quad p_D = \frac{K}{1+K}, \quad (3)$$

so that $K(p)$ and $K(T)$ can be determined from λ_N, λ_D, and the measured values of λ_{max} in the transformation range. Once K is known as a function of temperature or pressure, $\Delta G = G_D - G_N$ is determined from

$$\Delta G = -RT \ln K. \quad (4)$$

RESULTS

Figure 1 shows the fluorescence spectrum of Zn-Cc in the Q-band range at ambient temperature for a series of pressure levels between 100 MPa and 1 GPa. The band at 585 nm is the origin followed by a superposition of several vibrations around 640 nm. The sharp line structure around 695 nm is the fluorescence from a ruby crystal that is simultaneously recorded to determine the actual pressure level. As is obvious from the data, the pressure shift and broadening in the investigated range is rather moderate. Nevertheless it is clearly discernable that the Q band undergoes a blue shift at elevated pressure levels.

Figure 2 shows how band center λ_{max} and bandwidth w (FWHM) of the Q transition behave under a pressure variation up to ~1.5 GPa: The band center is almost insensitive to pressure variations up to ~600 MPa. Then, it undergoes a blue shift that covers a range of ~3 nm. Beyond ~1 GPa, the blue shift levels off again. The bandwidth increases steadily with pressure and reaches a maximum around 0.9 GPa. Then, it decreases again. The maximum of the broadening coincides with the midpoint of the range of the blue shift. The temperature of the experiment was 298 K.

Figure 3 shows the behavior of λ_{max} and w under a temperature variation at ambient pressure. The band center shifts moderately to the red up to temperatures of ~315 K.

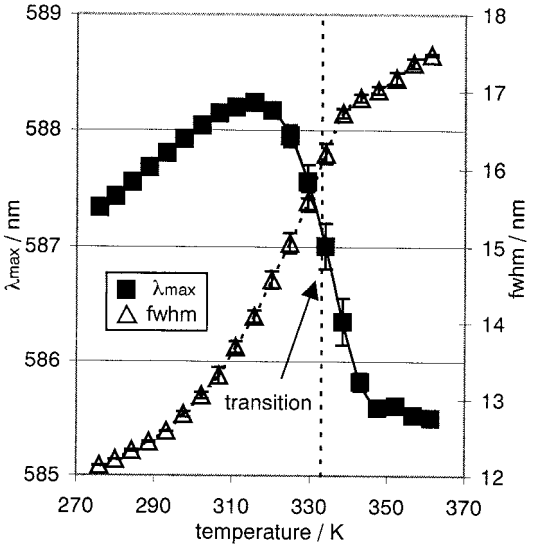

FIGURE 3 Center (λ_{max}) of the Q_x-Q_y-00-band and the respective width (FWHM) as a function of temperature at ambient pressure. The broken line marks the stability boundary.

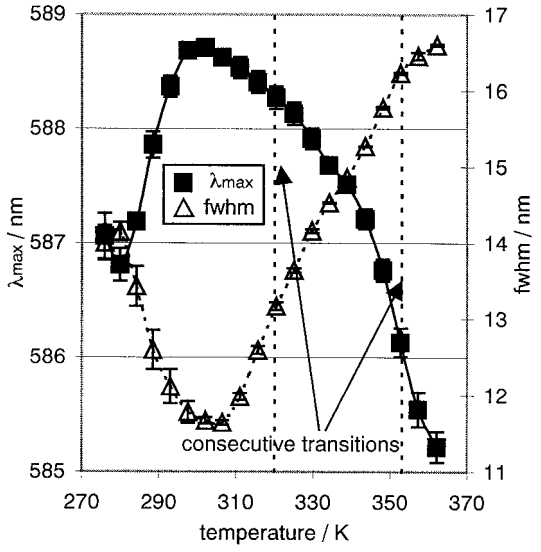

FIGURE 4 Center (λ_{max}) of the Q_x-Q_y-00-band and the respective width (FWHM) as a function of temperature at a pressure of 700 MPa.

The red shift is followed by a range with a pronounced blue shift, which levels off beyond 343 K. *w* steadily increases with temperature but, beyond the midpoint of the blue-shift range, the respective increase/Kelvin flattens.

Figure 4 serves as an example to demonstrate that the patterns of λ_{max} and *w* under pressure and temperature variations can be more complex. In this example, the temperature is varied at a pressure level of 700 MPa. The shift of the band center and, somewhat less pronounced, also the change of the bandwidth can be subdivided into three subranges. The range up to ~298 K is characterized by a rather pronounced red shift on the one hand and, somewhat unusual, a significant band narrowing, on the other hand. The range between 298 and 338 K is characterized by a blue shift and a broadening. Beyond 338 K, another range with a strong blue shift follows, which is also accompanied by a band broadening. The midpoint of this range is around 350 K. We attribute such a complex pattern to several, in this case two, consecutive steps in the denaturation process.

Figure 5 summarizes most of the pressure (*A*) and temperature (*B*) denaturation experiments. The data are represented as a function of the respective deviations from the transformation boundary $\Delta G = 0$, namely of $\lambda - \lambda_c$, $p - p_c$, and $T - T_c$, respectively. The index *c* characterizes the transformation boundary. p_c and T_c were determined from the midpoints of the blue-shift ranges and from the associated line-broadening patterns.

Figure 6 shows the stability diagram of the protein investigated. As can be seen, the shape of the diagram is ellipse-like. Note that, in the fluorescence pattern of Fig. 4, only the midpoint around 350 K fits into the diagram.

Figure 7 shows how we determined the edge values of the wavelengths λ_N and λ_D, which characterize the entrance to and the exit from the transformation range. We extrapolated the data of the respective ranges in a linear fashion. The respective cross points determine λ_N and λ_D, as described above. The data in Fig. 7 correspond with those in Fig. 3.

Figure 8 shows the difference $\Delta G = G_D - G_N$ as a function of pressure between 600 MPa and 1.1 GPa as determined from Eq. 4 and the measured wavelength of the band center (Eq. 2). The temperature is 298 K. The solid line represents a fit to a parabola whose first and second derivative yield the changes of the volume ΔV and the isothermal compressibility $\Delta\beta$, respectively.

Figure 9 is similar to Fig. 8. It shows ΔG as a function of temperature at ambient pressure. The first and second derivatives yield the changes in entropy and specific heat

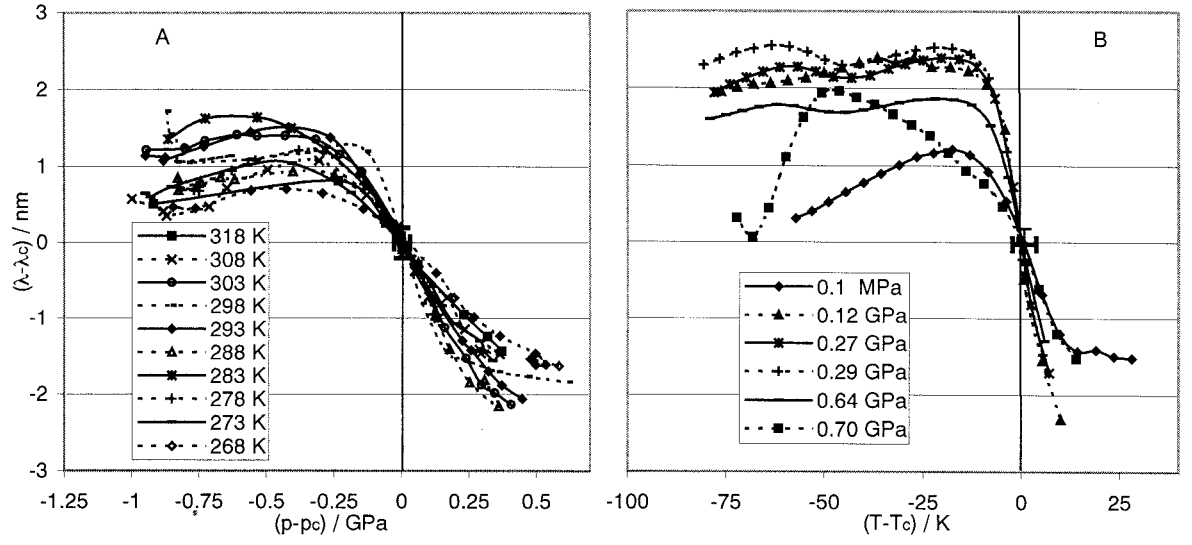

FIGURE 5 Summary of (*A*) pressure and (*B*) temperature denaturation data. λ_c, T_c, and p_c represent the wavelength, temperature, and pressure, respectively, at the stability boundary.

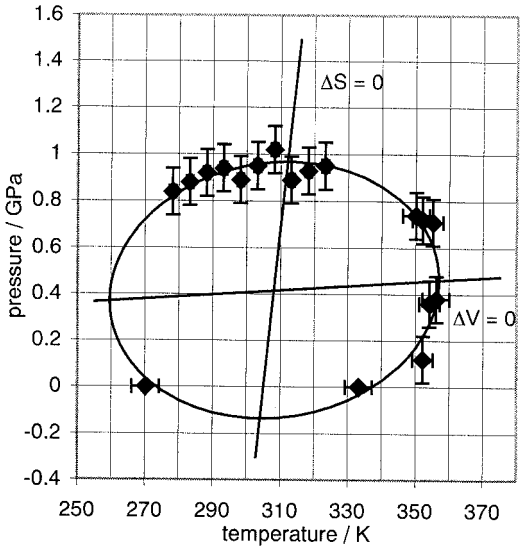

FIGURE 6 Stability diagram of Zn-Cc as obtained from the fluorescence experiments. The contour line represents a least-square fit of a second-order curve to the data points. The protein is stable inside the elliptic-like boundary. The outside range corresponds with the denatured state.

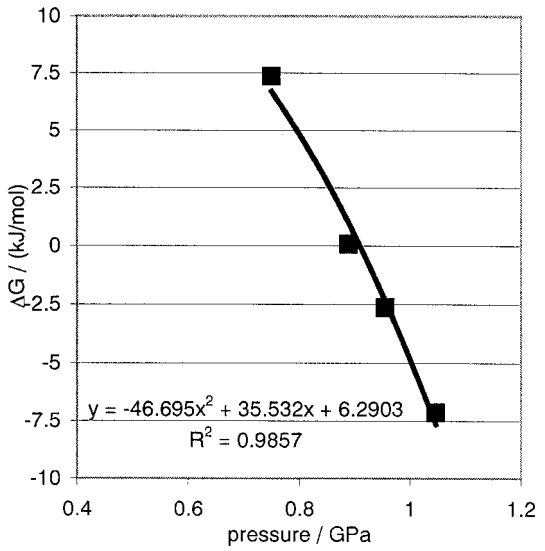

FIGURE 8 Difference of the Gibbs free energy ΔG as a function of pressure at a temperature of 298 K. The fit curve is a parabola.

capacity, ΔS and ΔC_p, respectively. Values of the thermodynamic parameters are summarized in Table 1.

DISCUSSION

The general pattern of the fluorescence and microscopic aspects of the transformation process

The interactions of a dye probe with its respective environment have been intensively studied in the past and are known in detail (for a review, see Israelachvili, 1994) so that it seems possible to extract information from the behavior of the fluorescence under changes of temperature and pressure on what is happening on a microscopic level during the unfolding process. The general pattern that we observe, e.g., for λ_{max}, is characterized by almost no changes or only a moderate red shift in the low pressure or temperature range. This range is followed by a pronounced blue-shift range, which again levels off at higher parameter values.

We first consider the behavior of the pressure shift. Proteins are ordered structures. Nevertheless they are characterized by an unusually large mean square displacement

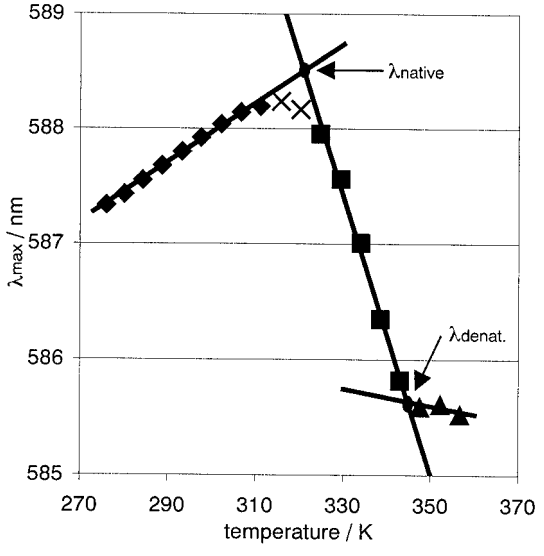

FIGURE 7 Determination of the edge values of λ_N and λ_D.

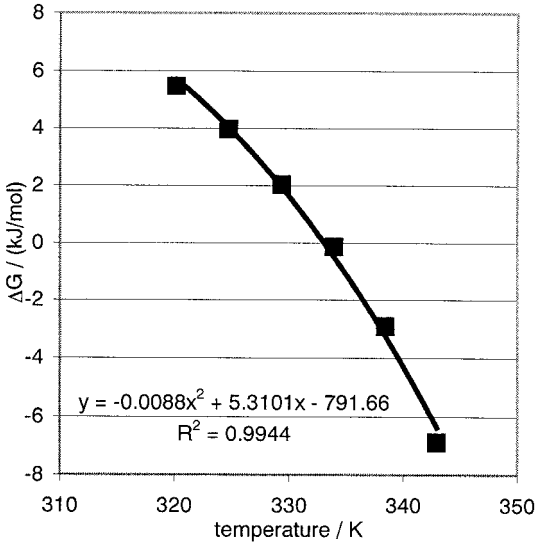

FIGURE 9 Difference of the Gibbs free energy ΔG as a function of temperature at ambient pressure. The fit curve is a parabola.

TABLE 1 Thermodynamic parameters for the denaturation of Zn-cytochrome *c*

Parameters	From the Fit	From Equilibrium Constant K
ΔC_p/(kJ mol^{-1} K^{-1})	—	5.87
$\Delta\beta$/(cm^3 mol^{-1} GPa^{-1})	−148.1	−93.4
$\Delta\alpha$/(cm^3 mol^{-1} K^{-1})	0.139	—
ΔV(0.91 GPa, 298 K)/(cm^3 mol^{-1})	−74.6	−49.4
ΔS(0.91 GPa, 298 K)/(kJ mol^{-1} K^{-1})	−0.263	—
ΔV(0.1 MPa, 333 K)/(cm^3 mol^{-1})	65.0	—
ΔS(0.1 MPa, 333 K)/(kJ mol^{-1} K^{-1})	0.530	0.556

For comparison, we list data obtained from the stability diagram and from the equilibrium constant, respectively.

$\langle x^2 \rangle$ (Frauenfelder et al., 1979, 1988; Parak et al., 1987) meaning that, as compared to organic crystals built from small molecules, there is an appreciable amount of structural disorder or, to put it differently, a large amount of structural freedom. Different local structures around a chromophore lead to a dispersion of the solvent shift, which shows up, for instance, as inhomogeneous line broadening (Laird and Skinner, 1989; Köhler et al., 1998). When pressure is applied, the density and, concomitantly, the magnitude of the intermolecular interactions increase. As a consequence, the magnitude and the dispersion of the solvent shift increase. However, concerning the magnitude of the pressure-modified solvent shift, it can be quite small, especially for aromatic molecules with polar groups (Zollfrank and Friedrich, 1992a,b; Gafert et al., 1993). The reason is that the solvent shift is a superposition of dispersive interactions and electrostatic interactions. Dispersive interactions lead always to a red shift because the polarizability in the excited state is always larger than in the ground state (Liptay, 1965). Electrostatic interactions, in contrast, usually cause a blue shift. (Note that tryptophan, which is quite often used as a fluorescence probe (e.g., Vidugiris et al., 1995, 1998; Jacob et al., 1999a,b; Panick et al., 1999) in unfolding experiments, is an exception. It has a very large dipole moment in the excited state as compared to the ground state, which induces a red shift). Hence, there is a partial compensation in the total shift that makes it small. For instance, we measured an average shift per pressure of ~1 nm/GPa for protoporphyrin IX-substituted myoglobin (Zollfrank et al., 1992). The small pressure changes, as shown, for instance in Fig. 2, fit into this scenario. In the pressure-induced dispersion of the solvent shift, however, there is no such compensation. Hence, the corresponding change in the pretransformation range is more pronounced (Fig. 2).

The flat range is followed by a range characterized by a significant blue shift of the order of a few nanometers. The shape of the curve has a sigmoid character, as clearly discernible in Figs. 2 and 5 *A*. From the sigmoid character, we conclude that the change in the shift pattern cannot just come from the increased density, but is rather based on a qualitative change of the microscopic interactions between probe and environment. This qualitative change occurs during a rather well-defined pressure range. Accordingly, we interpret this range as the range where the transformation from the native to the denatured state occurs. The fact that pressure induces a blue shift tells us that, in the transformation range, the relative weight of the electrostatic contribution to the solvent shift increases (Zollfrank and Friedrich, 1992a,b). Obviously, polar groups seem to come sufficiently close to the chromophore. This can happen in two ways: either the compact structure of the protein unfolds in a way so that the core of the pocket becomes exposed to the water molecules of the solvent, or water molecules of the solvent (i.e., of the hydration shell) are pressed into the interior of the protein. If this latter process takes place, the protein may retain its compact structure but may swell. There are several reasons that favor this second possibility. It is easily conceivable that an increasing isotropic pressure does not favor large-scale structural changes of the protein as would be the case if the protein interior were exposed to the solvent, because molecular groups had to be moved against a denser liquid. In addition, pressing water into the voids of the protein core is in line with a negative ΔV as obtained from Fig. 8, despite the fact that the protein may swell. The swelling may be overcompensated by the reduction of the volume of the hydration shell. The conclusion is that the observed blue shift of the fluorescence maximum fits well into the pressure unfolding scenario as suggested by Hummer et al. (1998a,b).

The shift of the band maximum under temperature variation, although it shows a similar pattern, is based on quite different processes. First, we stress that, as a rule, an increasing temperature always leads to a red shift if nothing unusual occurs. As the temperature increases, higher vibrational levels become progressively occupied so that the 00-transition is superimposed by the 11-, the 22-transitions, and so forth. Because the energy of the vibrational levels in the excited state is smaller than in the ground state, a progressive occupation of higher vibronic levels results in a red shift. This is exactly what we observe (Fig. 3). At zero pressure, this temperature-induced red shift is much more pronounced as compared to the corresponding pressure behavior. The reason for this is that, unlike the pressure shift, the temperature shift is not affected by a compensation mechanism.

Again, we associate the range of the blue shift with the transformation range to the unfolded state, and, as argued above, we attribute the occurrence of the blue shift to a qualitative change of the interaction of the chromophore with its nearby environment induced by an enhanced contribution from electrostatic terms that originate from a close contact with water molecules. This time, however, water molecules do not penetrate the protein. Instead, the interior of the protein unfolds in a way that it becomes exposed to

the solvent, as has been suggested by Baldwin and coworkers (Baldwin, 1986; Baldwin and Muller, 1992). Interestingly, the magnitude of the blue shift covers the same range for pressure and temperature variations. This finding tells us that the number of significantly interacting water molecules around the chromophore and their distance from it is roughly the same in both cases.

We conclude this section by stressing that pressure and temperature denaturation proceed along quite different microscopic pathways in the energy landscape of the protein, and it seems that the two processes do not lead to the same final state. A similar conclusion was drawn by Nash and Jonas (1997) on the basis of their high-pressure nuclear magnetic resonance work on lysozyme. They concluded that the cold denatured state resembles an early folding intermediate. How these findings may be reconciled with the "two-state approximation" will be discussed below.

Features of the line width

The behavior of the line width serves as an independent parameter to determine the midpoint of the transformation range, i.e., the stability boundary. As is obvious from Fig. 5, in some cases, it is difficult to determine this midpoint from the line shift behavior alone due to limitations in the experimentally accessible parameter range above the transformation boundary. Hence, it is very helpful to have a second observable to overcome this difficulty. Generally speaking, the midpoints as determined from the width w coincide quite well with the midpoints as determined from the shift (λ_{max}). Nevertheless, the width shows a few specific features that deserve a separate discussion. Figure 2 and all others in the respective series show that the line width broadens with increasing pressure, but, eventually, runs through a maximum (with which we associate the stability boundary). Beyond the maximum, there is a pressure regime where the band narrows significantly. In contrast, the behavior of the width with increasing temperature is different. There is no maximum and, consequently, no narrowing regime. However, the midpoint of the transformation range seems to be well characterized by a leveling off of the slope in the temperature broadening.

Line broadening under increasing pressure is a specific feature of disordered materials, e.g., liquids and glasses. The reason is that the structural correlation among the respective molecules is rather low. This low structural correlation is responsible for the fact that, as pressure is applied, the local conformations change and, as a consequence of that, the inhomogeneous band broadens. In crystals, for instance, where structural correlation is high, pressure mainly leads to a band shift but not to a pronounced band broadening (Gradl et al., 1992; Schellenberg et al., 1994). Along these lines of reasoning, it becomes clear that pressure broadening ceases beyond a level p_s where the density becomes sufficiently high so that structural correlation prevails. For proteins, this level can be estimated. If the displacement of an atom upon application of pressure is smaller than the root-mean-square displacement due to conformational disorder, $\langle x^2\rangle_c^{1/2}$, structural correlation is low. If it is larger, structural correlation is high, and there will not be much pressure broadening. $\langle x^2\rangle_c^{1/2}$ can be taken from low-temperature-extrapolated x-ray data. A reasonable number is 0.1 Å (Frauenfelder et al., 1979, 1988; Parak et al., 1987). Given a pressure-independent compressibility κ of the protein, we can estimate the pressure level p_s which leads, on average, to a displacement of the order of 0.1 Å simply from

$$\Delta a = \frac{a\kappa}{3} p_s, \tag{5}$$

with a being the average distance between the amino acid residues. With $\Delta a \approx 0.1$ Å, $\kappa = (-1/V)(\partial V/\partial p) \approx 0.1$ GPa^{-1} (Gekko and Noguchi, 1979; Gavish et al., 1983; Zollfrank et al., 1991; Friedrich, 1995; Friedrich et al., 1994) and $a \approx 3$ Å, we arrive at $p_s \approx 1$ GPa. That is, the pressure range where protein unfolding occurs for moderately low temperatures is already close to this critical value so that pressure broadening should already be suppressed through the rather high structural correlation.

Why, then, is there a maximum? As the transformation range is crossed, the denatured state becomes progressively populated. Hence, right at the stability boundary, we have an equal population of the native and the denatured state. The two states differ somewhat in their excitation energies. However, this difference is small as compared to the inhomogeneous width. Hence, the simultaneous excitation of the two states shows up as a broadening of the line. As pressure is increased beyond the stability boundary, the population of the native state ceases, and, because pressure itself does not produce a significant broadening anymore, the total line narrows again.

Of course, as we cross the transformation range by increasing the temperature, we, too, create a simultaneous population of the two states that contributes to the broadening of the fluorescence band. However, as we go beyond the stability boundary, narrowing cannot occur despite the fact that the population of the native state becomes less and less, because thermal line broadening, unlike pressure broadening, never leads to a saturation (at least as long as motional narrowing effects are absent). Accordingly, there is just a flattening in the respective slope (Fig. 3).

More complex patterns, reentrant transformations

At higher pressure levels, some of the line-shift and line-broadening data as a function of temperature show a more complex pattern (e.g., Figs. 4 and 5 *B*). λ_{max} shows two blue-shift phases of which the one at higher temperatures is more pronounced. These blue-shift phases are also reflected

in the behavior of the width. We interpret the blue-shift range at lower temperatures as kind of a pretransformation. We stress that such kinds of pretransformations are observed at rather high pressures, only. It is conceivable that, for water molecules to penetrate the protein pocket, other bonds have to be disrupted first. Note that, for pressures of ~1 GPa, the relative volume change is already of the order of 10%, and this change will preferentially affect the voids in or around the pocket so that water molecules cannot be pressed into these voids unless space is created by disrupting bonds.

In addition to these consecutive steps in the transformation process, Fig. 4 shows a rather peculiar initial phase in the temperature denaturation. λ_{max} undergoes a rather steep red shift (~2 nm/15 K), but, more peculiar, there is a significant line narrowing in the same temperature range. The most obvious reason for this behavior is the following. These data are taken at a pressure level of ~700 MPa. Inspection of Fig. 6 shows that around or below 275 K, this pressure level is very close to the stability boundary and, hence, we may have an almost equal population of the native and the denatured state. As we increase the temperature, we move into the more stable region of the diagram. Consequently, the denatured state relaxes back to the native state. As outlined above, the preferential population of just one state reduces the respective pressure broadening (and, in addition, compensates to some degree the thermal broadening) so that a net narrowing results. Because the denatured state is blue shifted as compared to the native state, back relaxation is accompanied by a comparatively strong red shift of the band maximum, as seen in the figure. In other words, the peculiar thermal behavior of the line shift and the bandwidth at high pressure levels is a consequence of the reentrant nature of the phase transformation of proteins where the stability boundary is crossed twice as the temperature is increased. These data demonstrate in a rather convincing way that folding and unfolding of Zn-Cc is a reversible process, even at rather low temperatures and high pressure levels.

The thermodynamics of unfolding of Zn-Cc

Provided the two-state model is a reasonable approximation for the unfolding–folding transformation and the process itself occurs sufficiently close to equilibrium, the equilibrium constant K can be determined from the spectroscopic data (Eq. 3). From K, ΔG can be determined. If ΔG is known along certain denaturation pathways in the (p, T) plane, e.g., along the p axis for certain temperature values T_i or along the T axis for certain pressure values p_i, it is a straightforward procedure to determine the complete set of thermodynamic parameters, namely $\Delta V(p, T_i)$, $\Delta S(T, p_i)$ and $\Delta\alpha$, $\Delta\beta$, and ΔC_p (Hawley 1971; Smeller and Heremans 1997; Heremans and Smeller 1998):

$$\left.\frac{\partial \Delta G}{\partial p}\right|_{T_i} = \Delta V(p, T_i), \qquad \left.\frac{\partial \Delta G}{\partial T}\right|_{p_i} = -\Delta S(T, p_i)\,, \tag{6}$$

$$\frac{\partial^2 \Delta G}{\partial p^2} = \Delta\beta, \quad T\frac{\partial^2 \Delta G}{\partial T^2} = -\Delta C_p, \qquad \frac{\partial^2 \Delta G}{\partial p \partial T} = \Delta\alpha\,. \tag{7}$$

As to such a procedure, however, there were experimental problems. Only in a few cases were we able to investigate the denatured state over a sufficiently large parameter range so that λ_D could be determined with sufficient accuracy. In most cases, we ran into limitations set either by the anvil cell or by the thermostat. Very reliable values for λ_D and λ_N were obtained for the temperature denaturation at ambient pressure (Fig. 7). Accordingly, we consider the associated value for ΔC_p also as highly dependable. ΔC_p was determined from the second derivative of a parabolic least-square fit through the respective ΔG values (Fig. 9). The parabola was constrained by the requirement that the two points, where it crosses the plane $\Delta G = 0$, had to coincide with the respective points of the stability diagram, namely at 270 and 333 K, respectively (Fig. 6). Note that, in this analysis, we did not take into account the slight rotation of the ellipse in the (p, T) plane as determined by the very small value for $\Delta\alpha$.

Because ΔC_p is considered to be a reliable value, we used it to determine the rest of the thermodynamic parameters from the stability diagram. The respective points have a rather high confidence level because they were determined from two independent quantities, namely the first and the second moment of the fluorescence. Hence, no extrapolation procedure was needed. In those cases where the transition to the denatured state could be seen in both quantities, the transformation boundaries coincided within a very narrow pressure or temperature range. In cases where we could not measure a leveling off of the line shift, the transformation boundary was determined from the respective behavior of the bandwidth, for instance, the cold denaturation transition at 270 K was identified through a pronounced minimum in the bandwidth. (Note that a decrease of the temperature is usually reflected in a narrowing of the bandwidth via its homogenous contribution. Whenever this narrowing runs through a minimum followed by a broadening regime, it signals the occurrence of a specific event that increases the heterogeneous contribution to the bandwidth. In our case, this event is the population of the denatured state whose absorption frequency differs from the respective one

of the native state. The behavior of the band shift in cold denaturation experiments is less characteristic in this case because both the thermal shift and the appearance of the denatured state cause a blue shift.) With ΔC_p known, all thermodynamic parameters can be determined from the stability diagram. In addition, the interesting values of ΔS and ΔV at any point of the transformation boundary can be determined from ΔC_p, $\Delta\beta$, and $\Delta\alpha$. Respective numbers are listed in Table 1.

For comparison, we also present $\Delta\beta_K$, the compressibility as obtained from the pressure dependence of the equilibrium constant K and, concomitantly, from ΔG. The respective data for $\Delta G(p)$ are shown in Fig. 8. The respective numbers coincide within a factor of 1.5. Again, we constrained the parabolic fit by the requirement that the $\Delta G = 0$ crossings coincided with the respective points in the stability diagram, namely with $p = 0.9$ and $p = -0.15$ GPa. Note that the latter point does not have any physical meaning.

The stability diagram shows the lines where ΔS and $\Delta V = 0$. ΔV is negative above a pressure of ~0.4 GPa. This is consistent with other data on pressure-induced unfolding of proteins (Kauzmann, 1987) and just reflects Le Chatelier's principle. As to ΔS, we expect it to be positive because the level of randomness is definitely larger in the unfolded structure. However, the stability diagram shows that this is true only if the temperature is above ~312 K. For the rest of the stability boundary, ΔS is negative. Still, however, the entropy of the denatured state must be larger than the respective one of the native state. Obviously, the negative entropy change must be due to the formation of an ordered structure in the solvent shell of the protein.

$\Delta\beta$ comes out negative, a result that is also reasonable. Note that $\Delta\beta = -V\Delta\kappa$, with κ being the compressibility in the usual definition. We expect the magnitude of the compressibility of a more random structure to be higher than the respective one of an ordered structure because there should be more free volume. Also, the order of magnitude of our value for $\Delta\beta$ compares well with literature data of other proteins (Hawley, 1971). We stressed above the high confidence level of ΔC_p. Indeed, our result is very close to what was measured for Cc by Privalov using calorimetric techniques (Privalov, 1979; Privalov and Gill, 1988; Makhatadze and Privalov, 1995). The calorimetric data are totally free of any model assumption (e.g., the two-state model). So we consider the coincidence of the spectroscopic and caloric result as an important support for the spectroscopic technique, which, as pointed out above, has to rely on several model assumptions. Note also that our Cc has a modified prosthetic group and the solvent in our experiment is a mixture of glycerol and water. Hence, the samples in our and in Privalov's experiment are not totally identical, a fact which might account for the small deviations of the data.

Comments on the two-state approximation: How confident is the stability diagram?

Finally we want to comment on the essential approximation on which the data analysis is based, namely on the two-state model. From the work of Kauzmann (1987), Baldwin (1986), and Hummer (1998a,b), and from the discussion above, it seems to be clear that pressure and temperature denaturation lead to different final states: the pressure-denatured state is a rather compact globule-like state, whereas the temperature denatured state may rather be kind of a random coil. However, viewing the unfolding process in an energy landscape picture (Frauenfelder et al., 1988, 1991) rather than in terms of two discrete states, pressure- and temperature-denatured states just represent different regions in a larger area of the complex energy landscape, which characterizes the denatured state in the sense that all respective phase-space coordinates represent structures in which the protein is not working. Similarly, the native state is also represented by a large area in conformation space reflecting those structures in which the protein is working. It seems possible to lump together these two phase-space areas to two effective states with a rather well-defined average energy so that an effective two-state model may be a well-working approximation. Of course, such a state lumping only works if the respective areas in phase space are not separated by too large barriers, which might prohibit a proper communication between them. We stress that similar energy-landscape views are also used in dynamic folding pictures (Dill and Chan, 1997).

SUMMARY

We investigated the stability diagram of Zn-cytochrome *c* as a function of pressure and temperature by using the shift and the width of the fluorescence origin as characteristic parameters. We found that the diagram has an ellipse-like shape. Based on the two-state model for proteins, it was possible to determine all relevant thermodynamic quantities that characterize the unfolding process. From the characteristic features in the behavior of the first moment as a function of pressure or temperature, it could be inferred that electrostatic contributions prevail during the transformation process. We interpreted this that either water is pressed into the protein pocket if pressure-induced denaturation occurs, or that the protein interior is exposed to the water molecules of the solvent, if temperature denaturation occurs. Although both procedures lead to different final states, we argued that an effective two-state model can be constructed that allows for an evaluation of the respective equilibrium constant, and, hence, for the whole set of thermodynamic quantities that determine the unfolding process.

We gratefully acknowledge financial support from the Deutsche Forschungsgemeinschaft (FOR 358, A1), from the Fond der Chemischen

Industrie and from the National Institutes of Health Grant RO1 GM55004 (J.M.V.).

REFERENCES

Baldwin, R. L. 1986. Temperature dependence of the hydrophobic interaction in protein folding. *Proc. Natl. Acad. Sci. U.S.A.* 83:8069–8072.

Baldwin, R. L., and N. Muller. 1992. Relation between the convergence temperatures T_h^* and T_s^* in protein unfolding. *Proc. Natl. Acad. Sci. U.S.A.* 89:7110–7113.

Clark, N. A. 1979. Thermodynamics of the re-entrant nematic-bilayer smectic A transition. *J. Physique Colloque.* C3:345–349.

Dill, K. A., and H. S. Chan. 1997. From Levinthal to pathways to funnels. *Nat. Struct. Biol.* 4:10–19.

Eremets, M. I. 1996. High Pressure Experimental Methods. Oxford University Press, Oxford, U.K.

Frauenfelder, H., F. Parak, and R. D. Young. 1988. Conformational substates in proteins. *Annu. Rev. Biophys. Chem.* 17:451–479.

Frauenfelder, H., G. A. Petsko, and D. Tsernoglou. 1979. Temperature-dependent x-ray diffraction as a probe of protein structural dynamics. *Nature.* 280:558–563.

Frauenfelder, H., S. G. Sligar, and P. G. Wolynes. 1991. The energy landscape and motions in proteins. *Science.* 254:1598–1603.

Friedrich, J. 1995. Hole burning spectroscopy and physics of proteins. *Methods Enzymol.* 246:226–259.

Friedrich, J., J. Gafert, J. Zollfrank, J. M. Vanderkooi, and J. Fidy. 1994. Spectral hole burning and selection of conformational substates in chromoproteins. *Proc. Natl. Acad. Sci. U.S.A.* 91:1029–1033.

Gafert, J., J. Friedrich, and F. Parak. 1993. A comparative pressure tuning hole burning study of protoporphyrin IX in myoglobin and in a glassy host. *J. Chem. Phys.* 99:2478–2486.

Gavish, B., G. Gratton, and C. J. Hardy. 1983. Adiabatic compressibility of globular proteins. *Proc. Natl. Acad. Sci. U.S.A.* 80:750–754.

Gekko, K., and H. Noguchi. 1979. Compressibility of globular proteins in water at 25°C. *J. Phys. Chem.* 83:2706–2714.

Gradl, G., A. Feis, and J. Friedrich. 1992. Pressure tuning of spectral holes in organic crystalline materials: irreversible effects. *J. Chem. Phys.* 97:5403–5409.

Hawley, S. A. 1971. Reversible pressure–temperature denaturation of chymotrypsinogen. *Biochemistry.* 10:2436–2442.

Heremans, K., and L. Smeller. 1998. Protein structure and dynamics at high pressure. *Biochim. Biophys. Acta.* 1386:353–370.

Hummer, G., S. Garde, A. E. Garcia, M. E. Paulalitis, and L. R. Pratt. 1998a. Hydrophobic effects on a molecular scale. *J. Phys. Chem. B.* 102:10469–10482.

Hummer, G., S. Garde, A. E. Garcia, M. E. Paulalitis, and L. R. Pratt. 1998b. The pressure dependence of hydrophobic interactions is consistent with the observed pressure denaturation of proteins. *Proc. Natl. Acad. Sci. U.S.A.* 95:1552–1555.

Israelachvili, J. N. 1994. Intermolecular and Surface Forces. Academic Press, London.

Jacob, M., M. Geeves, G. Holtermann, and F. X. Schmid. 1999a. Diffusional barrier crossing in a two-state protein folding reaction. *Nat. Struct. Biol.* 6:923–926.

Jacob, M., G. Holtermann, D. Perl, J. Reinstein, T. Schindler, M. A. Geeves, and F. X. Schmid. 1999b. Microsecond folding of the cold shock protein measured by a pressure jump technique. *Biochemistry.* 38:2882–2891.

Kauzmann, W. 1987. Thermodynamics of unfolding. *Nature.* 325: 763–764.

Köhler, M., J. Friedrich, and J. Fidy. 1998. Proteins in electric fields and pressure fields: basic aspects. *Biochim. Biophys. Acta.* 1386:255–288.

Laird, B. B., and J. L. Skinner. 1989. Microscopic theory of reversible pressure broadening in hole-burning spectra of impurities in glasses. *J. Phys. Chem.* 90:3274–3281.

Liptay, W. 1965. Die Beeinflussung der optischen Absorption von Molekülen durch ein äuβeres elektrisches Feld. III. Berücksichtigung der direkten Feldstärkeabhängigkeit des Übergangsmoments und des inneren Feldes in einer Lösung. *Z. Naturforsch.* 20a:272–289.

Makhatadze, G. I., and P. L. Privalov. 1995. Energetics of protein structure. *Adv. Protein Chem.* 47:307–425.

Nash, D. P., and J. Jonas. 1997. Structure of pressure-assisted cold denatured lysozyme and comparison with lysozyme folding intermediates. *Biochemistry.* 36:14375–14383.

Panick, G., G. J. A. Vidugiris, R. Malessa, G. Rapp, R. Winter, and C. A. Royer. 1999. Exploring the temperature–pressure phase diagram of staphylococcal nuclease. *Biochemistry.* 38:4157–4164.

Parak, F., H. Hartmann, K. D. Aumann, H. Reuscher, G. Rennekamp, H. Bartunik, and W. Steigemann. 1987. Low temperature x-ray investigation of structural distributions in myoglobin. *Eur. Biophys. J.* 15: 237–249.

Privalov, P. L. 1979. Stability of proteins. *Adv. Prot. Chem.* 33:167–241.

Privalov, P. L., and S. J. Gill. 1988. Stability of protein structure and hydrophobic interaction. *Adv. Prot. Chem.* 39:191–234.

Schellenberg, P., J. Friedrich, and J. Kikas. 1994. Spectral hole burning in polymorphic systems: single site pressure phenomena and glassy behavior. *J. Chem. Phys.* 100:5501–5507.

Smeller, L., and K. Heremans. 1997. Some thermodynamic and kinetic consequences of the phase diagram of protein denaturation. *In* High Pressure Research in the Biosciences and Biotechnology. Leuven University Press, Leuven, Belgium. 55–58.

Vanderkooi, J. M., F. Adar, and M. Erecinska. 1976. Metallocytochrome *c*: characterization of electronic and emission spectra of Sn and Zn cytochromes *c*. *Eur. J. Biochem.* 64:381–387.

Vidugiris, G. J. A., J. L. Markley, and C. A. Royer. 1995. Evidence for a molten globule-like transition state in protein folding from determination of activation volumes. *Biochemistry.* 34:4909–4912.

Vidugiris, G. J. A., and C. A. Royer. 1998. Determination of the volume changes for pressure-induced transitions of apomyoglobin between the native, molten globule, and unfolded states. *Biophys. J.* 75:463–470.

Zipp, A., and W. Kauzmann. 1973. Pressure denaturation of metmyoglobin. *Biochemistry.* 12:4217–4228.

Zollfrank, J., J. Friedrich, J. Fidy, and J. M. Vanderkooi. 1991. Photochemical hole under pressure: compressibility and volume fluctuations. *J. Chem. Phys.* 94:8600–8603.

Zollfrank, J., and J. Friedrich. 1992a. Pressure shift and solvent shift: a hole-burning study of resorufin-doped glasses. *J. Phys. Chem.* 96: 7889–7895.

Zollfrank, J., and J. Friedrich. 1992b. Spectral holes under pressure: proteins and glasses. *J. Opt. Soc. Am. B.* 9:956–961.

Zollfrank, J., J. Friedrich, and F. Parak. 1992. Spectral hole burning study of protoporphyrin IX substituted myoglobin. *Biophys. J.* 61:716–724.